Do Photobleached Fluorescent Microtubules Move?: Re-evaluation of Fluorescence Laser Photobleaching both In Vitro and in Growing *Xenopus* Axon

Shigeo Okabe and Nobutaka Hirokawa

Department of Anatomy and Cell Biology, School of Medicine, University of Tokyo, Hongo, Tokyo, 113 Japan

Abstract. We previously documented differences in the behavior of microtubules in growing axons of two types of neurons, adult mouse sensory neurons and *Xenopus* embryonal spinal cord neurons. Namely, the bulk of microtubules was stationary in mouse sensory neurons both by the method of photoactivation of caged-fluorescein-labeled tubulin and photobleaching of fluorescein-labeled tubulin, but the bulk of microtubules did translocate anterogradely by the method of photoactivation. Although these results indicated that the stationary nature of photobleached microtubules in mouse neurons is not an artifact derived from the high levels of energy required for the procedure, it has not yet been settled whether the photobleaching method can detect the movement of microtubules properly.

Here we report photobleaching experiments on growing axons of *Xenopus* embryonal neurons. Anterograde movement of photobleached microtubules was observed at a frequency and translocation rate similar to the values determined by the method of photoactivation. Our results suggest that, under appropriate conditions, the photobleaching method is able to reveal the behavior of microtubules as accurately as the photoactivation method.

THE recently developed technique of microinjection of cytoskeletal proteins tagged with various kinds of hapten or fluorescent derivatives provided us with considerable information about the dynamic distribution and mode of turnover of the cytoskeletal polymers in living cells. One possible approach for monitoring the dynamics of the cytoskeletal proteins is to visualize single fluorescent polymers in real time (Sammak and Borisy, 1988*a*). Although this method enabled us to reveal some important dynamic features of cytoskeletal proteins such as the assembly-disassembly process of microtubules (MTs)[1] in interphase cells (Sammak and Borisy, 1988*b*; Schulze and Kirschner, 1988), the requirement of a sparse distribution of polymers at the cellular domains of interest restricted the possible application of this technique to other dynamic assemblies such as mitotic spindles or the neuronal cytoskeleton. Alternatively, it is possible to determine the incorporation and successive assembly of the cytoskeletal proteins by injecting hapten-labeled proteins and successive fixation and immunolabeling (Soltys and Borisy, 1985; Schulze and Kirschner, 1986; Okabe and Hirokawa, 1988). However, this technique inherently involves the possibility of disturbing the native cellular conditions by any injection trauma and by the increase of free subunits introduced abruptly.

There remain two possible approaches for monitoring the turnover of cytoskeletal proteins, both of which are promising since they visualize the turnover at a steady state regardless of the density of the cytoskeletal polymers at the cellular region of interest. One is the fluorescence recovery after photobleaching, where a discrete bleached zone generated by an intense light source is analyzed for its movement and recovery of fluorescence (Saxton et al., 1984; Sammak et al., 1987; Kreis et al., 1982). The other method, which seems to be a reversal of the photobleaching technique, is the photoactivation of proteins labeled with caged fluorescent molecules (Mitchison, 1989). Here, illumination with a UV microbeam releases fluorescent molecules from their "cage" and generates a discrete fluorescent zone against a dark background. Although it had been hoped that the behavior of the cytoskeletal proteins as revealed by these two distinct methods would be identical and the two methods could therefore be used interchangeably, considerable disagreement has recently surfaced regarding the behavior of tubulin molecules (Gorbsky et al., 1988; Mitchison, 1989; Okabe and Hirokawa, 1990; Lim et al., 1990; Reinsch et al., 1991).

In particular, the discrepancies between the two techniques have not been insignificant in the case of the behavior of MTs in the axon of nerve cells. A major issue on the mechanism of establishing the neuronal cytoskeleton along the extremely long axon (Hirokawa, 1982, 1991) is whether the unit of active transport of tubulin is the MTs themselves or free oligomeric tubulin molecules (Lasek, 1986; Okabe and Hirokawa, 1989; Hollenbeck, 1989). Initially, pulse-labeling

1. *Abbreviations used in this paper*: MT, microtubule; NHS-Fl, 5(6)-carboxy-fluorescein succinimidyl ester; NHS-XRh, 5(6)-carboxy-X-rhodamine succinimidyl ester.

studies did raise the hypothesis that tubulin molecules were assembled in the cell body and traveled down the axon as polymers (Black and Lasek, 1980; Lasek, 1986). In contrast, studies using the technique of photobleaching fluorescent MTs in the axon of mouse and chick neurons reported quite a different picture—namely, MTs marked by photobleaching did not move during the period of significant growth of the axon, indicating that MT polymers are stationary and free oligomeric tubulins are the unit of transport (Okabe and Hirokawa, 1990; Lim et al., 1990). Unfortunately, this view was not supported by the recent photoactivation study on *Xenopus* embryonal neurons. When a small region of growing axons of *Xenopus* neurons was photoactivated to generate a fluorescent mark, anterograde movement of this mark was repeatedly observed, supporting the idea of en bloc movement of MTs in the axon (Reinsch et al., 1991). Since the data of photoactivation on *Xenopus* neurons strongly contrast with the results of photobleaching on chick and mouse neurons, and whether MTs do move or not is the fundamental question to be resolved, it would appear necessary to determine whether the observed marked discrepancy is the result of some technical artifacts or is inherent to the nature of the different neuron types used in these studies.

To clarify this point, we previously reported the behavior of photoactivated MTs in both mouse and *Xenopus* neurons and observed no movement of photoactivated MTs in mouse axons (Okabe and Hirokawa, 1992). Although those results indicated that the stationary nature of photobleached MTs in mouse neurons is not an artifact derived from the high levels of energy required for photobleaching, it has not yet been settled whether the photobleaching method can detect the movement of MTs in *Xenopus* axon properly. In this study, we first determined the intensity range of laser irradiation by which MTs were sufficiently bleached to be distinguishable from unbleached MTs, but without causing any deteriorative effects in vitro. Under this condition, we could observe the anterograde movement of photobleached MTs at a frequency and translocation rate similar to those determined by the method of photoactivation. Our results suggest that, when carefully controlled, photobleaching and photoactivation techniques can report the behavior of cytoskeletal proteins similarly and interchangeably.

Materials and Methods

Preparation of Fluorescein- or X-rhodamine-labeled Tubulin

Phosphocellulose-purified hog brain tubulin was labeled with 5(6)-carboxyfluorescein succinimidyl ester (NHS-Fl) and 5(6)-carboxy-X-rhodamine succinimidyl ester (NHS-XRh) (Molecular Probes Inc., Junction City, OR) according to the method of Kellog et al. (1988). The molar f-to-p ratio of the final product was estimated by measuring the protein concentration and dye concentration with a spectrophotometer using the extinction coefficients of 48,000 at 490 nm for NHS-Fl and 70,000 at 590 nm for NHS-XRh.

Polymerization of MTs for In Vitro Photobleaching

NHS-Fl-labeled tubulin, NHS-XRh-labeled tubulin, and unlabeled tubulin at 10, 40, and 30 μM, respectively, were polymerized in PEM buffer (80 mM K-Pipes, pH 6.8, 1 mM $MgCl_2$, 1 mM EGTA) plus 4 mM $MgCl_2$, 30% glycerol, and 1 mM GTP at 37°C for 30 min. MTs were diluted in PEM buffer plus glycerol and taxol to final concentrations of 0.2 mg/ml of MTs, 5% glycerol, and 10 μM taxol. Since the molar f-to-p ratio of both NHS-Fl-labeled tubulin and NHS-XRh-labeled tubulin was 0.8, the final f-to-p ratio of NHS-Fl- and NHS-XRh-labeled tubulin was estimated to be 0.1 and 0.4, respectively.

Optics

Fluorescence imaging was performed with an Olympus IMT-2 inverted microscope (Olympus Corp., Lake Success, NY) and a Nikon X100 fluor objective lens (1.3 NA; Nikon Inc., Melville, NY) (see Fig. 1). 50-W halogen lamps were used for trans- and epi-illumination. A 488-nm beam generated by an argon ion laser (GLS-3050; NEC, Tokyo, Japan) was introduced into the light path for epi-illumination by inserting a beam splitter between the original mirror box and the halogen lamp. A cylindrical lens was positioned between an electronic shutter and the beam splitter to produce a focused beam in the specimen plane. For photobleaching experiments on *Xenopus* neurons, images were projected to an image intensifier coupled with a CCD camera (C2400-87; Hamamatsu Photonics, Hamamatsu, Japan). For in vitro photobleaching experiments, images were projected to an SIT camera (C2400-08; Hamamatsu Photonics) because the SIT camera had higher resolutions for detecting single MTs in our experimental condition. Video frames were summed and averaged for 0.5–1 s, and the background fluorescence was subtracted with a digital image processor (ARGUS-10, or ARGUS-100; Hamamatsu Photonics). Images were stored on tape using an SP.U-matic video cassette recorder (model VO-9600; SONY, Tokyo, Japan).

Observation of Fluorescent MTs In Vitro

To observe fluorescent MTs in vitro, 1.5 μl of the solution of fluorescent MTs was squashed between a coverslip and a slide glass. To prevent the sample from drying, the assembly was sealed with silicon grease. The thickness of the chamber was estimated to be 5 μm, since 1.5 μl of the solution fully spread over an area of 3 cm^2. Single fluorescent MTs were able to be detected with epi-illumination for 1 s through a rhodamine filter set. At least 10 frames of the same field could be recorded without any detectable damage to the MT structure. Usually, we restricted the illumination to <5 s, and images before and at 0, 5, and 10 min after photobleaching were obtained. Images of MTs 10 min after photobleaching were used to determine the damage to MTs, since the images at this time point always presented the damage most clearly. The images showing dissolution of more than half of the MTs in bleached zones were scored as 100, and the images containing no aberrant MTs were scored as 0. The remaining images, namely those with less than half of the MTs damaged, were given a score of 50. The average of 20 photobleaching runs with four different samples was calculated as the index of the extent of MT breakage at a given irradiation condition.

Introduction of Fluorescent Tubulin and Culture of Xenopus Embryos

Xenopus embryos were fertilized, injected, incubated, and dissected as described previously with the following modifications (Okabe and Hirokawa, 1992). We used NHS-Fl-labeled tubulin at a concentration of 5–10 mg/ml. At stages 22–25, injected embryos were examined under epi-illumination with blue light and heavily labeled embryos were further processed for culture.

Photobleaching of Xenopus Neurons

The fluorescent cells were positioned with the aid of a mark on a monitor. A focused laser beam (peak intensity of 2.7 mega watt/m^2 and a half-width of 3.3 μm at 1/10 intensity) was applied to the sample for 1/30 s to produce a photobleached mark on the fluorescent axon. Between the acquisition of fluorescent images, phase-contrast images of the same field were recorded at intervals of 10–15 min to confirm that the position of the cell body did not move. Only neurons which did not change position of the cell body and direction of the axon were further used for the translocation rate measurements of photobleached zones.

Image Analysis

Digitized images of fluorescence microscopy were quantified with an image processor (ARGUS-100; Hamamatsu Photonics). Using an argon ion laser coupled to a laser power meter and neutral density filters, a series of light intensities was generated to illuminate a standard fluorescein sample, and the linearity of both the ICCD and SIT cameras was checked. Within the range of the fluorescence intensity of our sample (0–5,000 per pixel), the

output of both cameras was linear. For line intensity measurements, a horizontal zone was superimposed on the axon and the average of fluorescence intensities across each longitudinal row of pixels was calculated and plotted against the distance from the left side of the zone. The movement of photobleached spots was calculated from the position of the bottom of the fluorescence intensity for each intensity profile. The width of the bleached spot was determined by measuring the distance between two points which were at positions of half of the intensity between the maximum and minimum values.

Results

Tubulin Labeling with Fluorescein

In this study we chose NHS-Fl for labeling tubulin. There were two reasons for this choice of label. First, this chromophore has been used in our laboratory to monitor the dynamics of MTs in neurons, and a direct comparison of the present analysis with the previous one would be possible (Okabe and Hirokawa, 1990). Second, the effects of photobleaching on tubulin molecules labeled with the identical chromophore have previously been studied by Vigers et al. (1988), and the energy required to promote MT breakage has already been reported. This enabled us to restrict our photobleaching conditions to the energy range reported to be safe for labeled MTs in vitro.

We labeled tubulin with NHS-Fl according to the method of Kellog et al. (1988), and the f-to-p ratio of the product was estimated to be 0.8–0.9. This labeled tubulin showed similar rates of assembly in vitro compared with unlabeled tubulin, and was incorporated into the MT network in living fibroblasts and neurons in a normal manner (Okabe and Hirokawa, 1990).

Optical System

We used basically the identical optical system for photobleaching as that used in our previous reports on mouse sensory neurons (Okabe and Hirokawa, 1990, 1991). Fig. 1 shows a diagram of the apparatus. Without a cylindrical lens inserted between the electronic shutter and a beam splitter, the 488-nm line of an argon ion laser produced a beam with a disk cross section of a diameter of 62 μm at 1/10 intensity in the specimen plane. With a cylindrical lens, the cross section of the beam in the specimen plane was a bar of a half width of 3.3 μm at 1/10 intensity. To determine the relative intensity of the 488-nm beam in the specimen plane under these two conditions, we measured peak values of fluorescence intensities of fluorescein standards illuminated with an argon ion laser attenuated with neutral density filters. The peak intensity of the beam with a cylindrical lens was determined to be 4.6-fold higher than that without a cylindrical lens. Using a laser power meter, the intensity of laser irradiation was measured. When the argon ion laser was operated at the minimum output, which was the condition used for the in vivo study described later, the intensity at the positions 1 and 2 in Fig. 1 was 1.16 mW and 0.56 mW, respectively. By integrating the intensity profile of the beam without a cylindrical lens and calculating the mean of the light intensity, we estimated the peak of the light intensity without a cylindrical lens to be 590 kW/m^2. From this value, the peak of the light intensity with a cylindrical lens was calculated to be 2.7 MW/m^2.

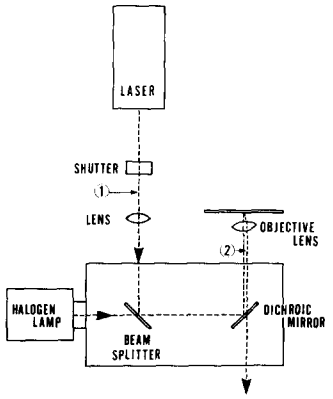

Figure 1. Diagram of the photobleaching system. See Materials and Methods and the Optical System Section in the Results section for details.

Effect of Photobleaching on MTs Assembled In Vitro

Vigers et al. (1988) reported previously that MTs labeled with NHS-Fl broke up with a 488-nm light from an argon ion laser at the intensity range of 0.5–150 MW/m^2. Our illumination conditions (−3 MW/m^2) were at the lowest dose, and Vigers et al. (1988) presented no data on the effects of short-time irradiation (<10 s) at such relatively low light intensity, and thus we planned to study the effects of short-time irradiation at low light intensity on MTs labeled with NHS-Fl in vitro.

We planned to carry out both in vitro and in vivo experiments with the same microscope, since precise control of the illumination dose would be possible using the identical optical system. However, the microscope we have used for the photobleaching can not be equipped with DIC or darkfield optics, which are necessary to visualize MTs without the aid of fluorescent probes, and we could not apply the method described by Vigers et al. (1988) to monitor the breakage of MTs in vitro. Instead, we polymerized MTs from a mixture of fluorescein- and X-rhodamine–labeled tubulin and visualized their fluorescent images through an SIT camera by illumination with a green light. To avoid the possible effect of resonance transfer from fluorescein to rhodamine fluorophore during irradiation (Herman, 1989), we used tubulin labeled with X-rhodamine, which has a longer excitation wave length (570 nm) and does not work as an energy acceptor. As expected, we observed no fluorescence quenching when X-rhodamine tubulin was co-polymerized with NHS-Fl tubulin.

Fluorescent MTs were polymerized in PEM buffer containing 10 μm taxol and 5% glycerol and were then observed at 26°C. The final concentration of MTs was 0.2 mg/ml and the f-to-p ratios of fluorescein and rhodamine were 0.1 and 0.4, respectively. The f-to-p ratio of 0.1 was chosen for fluorescein because this value was close to the f-to-p ratio of the labeled MTs to be photobleached in cells (Okabe and Hirokawa, 1988). These conditions were similar to those of Vigers et al. (1988) except that the concentration of MTs was much lower in our experiments to prevent the overlap of individual fluorescent MTs. As shown in Fig. 2, we could visualize single MTs under these conditions and follow the structure of MTs after illumination with an intense blue light. To bleach MTs in vitro, we used a laser beam without focusing with a cylindrical lens, since the lateral movement of MTs out of the narrow, focused bleach zone during the observation made it difficult to judge MT breakage. The beam

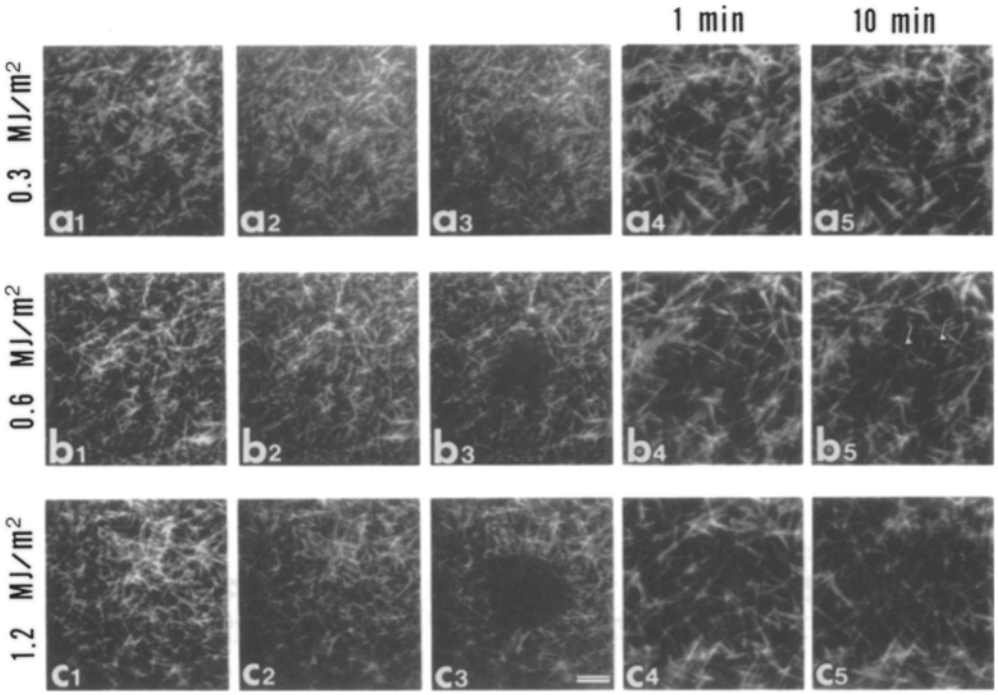

Figure 2. Photobleaching of taxol-stabilized MTs in vitro. MTs containing NHS-Fl and NHS-XRh-labeled tubulin with an f-to-p ratio of 0.1 and 0.4, respectively, were photobleached with a light energy of 0.3 (*a*), 0.6 (*b*), and 1.2 (*c*) MJ/m². Fluorescein images were obtained just before (*a2* to *c2*) and after bleaching (*a3* to *c3*) to monitor the degree of photobleaching. Rhodamine images were recorded before (*a1* to *c1*) and 1 min (*a4* to *c4*) and 10 min (*a5* to *c5*) after bleaching to determine whether MTs were photodamaged. Frames *4* and *5* are presented at higher magnification to show the morphology of single fluorescent filaments. With an exposure of 0.6 MJ/m², breakage of a few MTs was observed (*arrows* in *b5*), but as the irradiation increased, images of aberrant MTs increased (*c5*). Bar: (Frames 1–3) 10 μm; (frames 4 and 5) 2.5 μm.

without a cylinder lens illuminated a circular area with a diameter of 60 μm at two light intensities whose peak values were 0.59 and 2.7 MW/m². The latter, 2.7 MW/m², corresponded to the peak intensity of the focused beam used for photobleaching fluorescent MTs in *Xenopus* neurons, which will be described later.

We first determined the degree of photobleaching after irradiation with an argon ion laser, with the exposure time varying from 8 msec to 2 s. Fig. 3, *A* and *B* show the plot of fluorescence intensity against exposure time at two different laser intensities. Each point represents the average of 20 measurements of four different samples, and the SEM for each point varied from 0.5 to 2.6. As exposure time increased, rapid bleaching of fluorescence was observed. When the fluorescence intensity was plotted against the total dose of irradiation (namely, laser intensity × exposure time), the curves of photobleaching were similar at two different laser intensities (Fig. 3 *C*), suggesting that the total dose of irradiation mainly determines the degree of photobleaching under this condition. If photobleaching of the fluorophore to a nonfluorescent one is a simple irreversible first-order reaction, the concentration of the unbleached fluorophore (C[t]) after photobleaching lasting a time interval t is given by

$$C(t) = Co \times \exp(-\alpha It)$$

where Co is the initial concentration of the fluorophore, and I is the bleaching intensity (Axelrod et al., 1976). To determine whether the experimental data fit this theoretical equation, we made a semi-log plot of the fluorescence intensity (Fig. 3 *D*). Since the experimental data did not form straight lines intercepting the ordinate at a value of 100%, the process of photobleaching fluorescent MTs can not be explained by simple irreversible first-order reaction.

Next, we observed the structures of MTs at several time points after photobleaching (Fig. 2) and scored the extent of MT breakage by the criteria described in Materials and Methods. We illuminated MTs for various irradiation times at two intensities, followed the structure of MTs at 1 and 10 min after bleaching, and plotted the extent of MT breakage against the total dose of irradiation (Fig. 4, *A* and *B*). This plot shows that MTs were intact when laser illumination lasted for <1/4 s and <1/15 s at a peak laser intensity of 0.59 and 2.7 MW/m², respectively. It is probable, as in the case of the degree of photobleaching, that the total dose of irradiation mainly determines whether MTs remain intact or are damaged, since the two experimental curves of MT breakage under different irradiation intensities fit very well when plotted against the total dose of irradiation (Fig. 4). To test the possibility that MTs take a longer time (>10 min) to break when illuminated at a lower dose, we followed MTs which had been irradiated with a total dose of 0.2 mega joule/m² up to 60 min after bleaching. No breakage was observed, and any structural damage on MTs seems to become evident within 10 min after illumination.

From Fig. 3 *C* and 4, we can estimate the exposure which is not destructive to fluorescent MTs as well as the degree of bleaching with the given exposure. The total energy of exposure ranging from 0.05 to 0.09 MJ/m² seems to be adequate for photobleaching, since this exposure is tenfold less than the exposure to cause MT breakage and can decrease fluorescence intensity to 50% of the original value. Therefore, we chose an exposure of 1/30 s at a laser power of 1.16 mW with a cylindrical lens (which produces a peak intensity

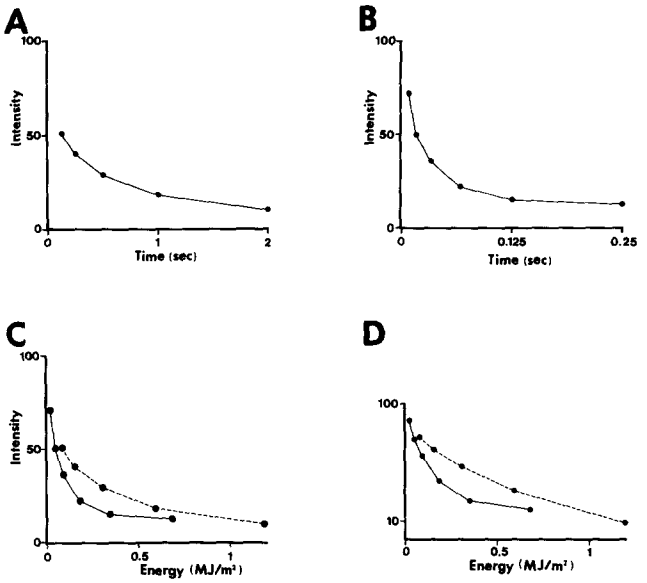

Figure 3. The degree of fluorescence photobleaching plotted against time and total energy. (*A* and *B*) Fluorescence intensity in bleached regions plotted against exposure time at two laser intensities of 0.59 (*A*) and 2.7 (*B*) MW/m² (the peak intensity). (*C*) Fluorescence intensity in bleached regions plotted against total energy at two peak laser intensities of 2.7 (*solid line*) and 0.59 (*dotted line*) MW/m². The degree of photobleaching is similar at the two light intensities. (*D*) Fluorescence intensity in bleached regions presented as a semi-log plot at two peak laser intensities of 2.7 (*solid line*) and 0.59 (*dotted line*) MW/m². Assuming that fluorescence bleaching is a simple irreversible first-order reaction, the degree of photobleaching would be on the straight lines which intercept the ordinate at the value of 100%. The experimental data which are not on these lines suggest that the process of photobleaching can not be explained by simple irreversible first-order reaction.

of 2.7 MW/m² and a peak energy applied during the exposure of 0.09 MJ/m²) for the in vivo bleaching experiment described in the following section.

Photobleaching of Fluorescent MTs in Growing Xenopus *Axons*

Anterograde movement of photoactivated MTs has been reported in growing axons of *Xenopus* embryonal neurons (Reinsch et al. 1992; Okabe and Hirokawa, 1992). To analyze the behavior of photobleached MTs in *Xenopus* neurons, we introduced NHS-Fl labeled tubulin into *Xenopus* embryos at the two-cell stage, allowed them to develop to stages 22–25, and isolated spinal cord neurons for dissociation culture. The growing neurites of these cells contained fluorescent MTs, and photobleaching experiments were performed 2–10 h after plating. The conditions for tubulin injection, cell culture, the time course of making fluorescent marks and the subsequent observations were identical to our previous photoactivation experiment (Okabe and Hirokawa, 1992). As stated previously, the condition of exposure to a focused laser beam (peak intensity of 2.7 MW/m² for 1/30 s) was the value proven to have no destructive effect on the MT structure in vitro.

When a narrow region of rapidly extending fluorescent axons was photobleached with an argon ion laser, we frequently observed anterograde movement of the photobleached

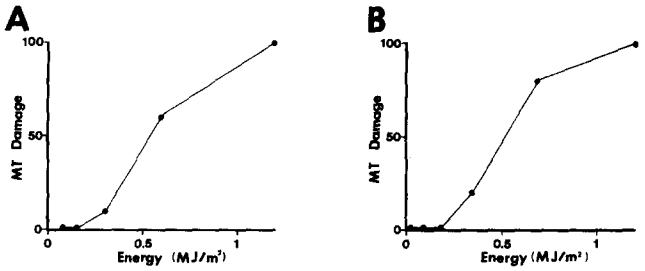

Figure 4. The extent of MT breakage plotted against total energy exposed to MTs at two different peak light intensities of 0.59 (*A*) and 2.7 (*B*) MW/m². The method of determining the extent of MT breakage is stated in Materials and Methods.

zones. Fig. 5 shows an example of the photobleaching experiments. This neuron had a short, sprouting axon and the whole structure of the neuron was visualized by epi-illumination. By application of a focused laser beam, a dark spot was generated on the fluorescent axon and its behavior was followed intermittently. As the axon became elongated, the bleached spot translocated distally. The anterograde movement of the bleached spot was considerably slower than that of the growth cone, and the length both between the growth cone and the bleached spot and between the bleached spot and the cell body increased significantly with time. Fig. 6 shows another example of the anterograde translocation of photobleached spots. In this case, the axon was longer than that presented in Fig. 5 but elongated at a similar rate. Movement of the bleached spot down the axon was clearly observed after photobleaching.

The translocation of photobleached zones was a repeatedly observed phenomenon. Of 36 photobleaching experiments using rapidly growing axons, 21 photobleached zones (58.3%) showed forward movement. To measure the translocation rate, we created fluorescence intensity profiles along the axons shown in Fig. 5 and 6. The troughs on fluorescence intensity profiles (arrows in Fig. 5 *J* and 6 *H*) changed their position toward the right of the figures with time, confirming the movement of the photobleached region along the axon. The fluorescence intensity profiles also indicate that the recovery of fluorescence in the bleached zones occurs gradually with a recovery half-time of 10 to 20 min. This rate of fluorescence recovery fits well with our previous photoactivation study which reported a significant decay of photoactivated signals within 20 min after photoactivation (Okabe and Hirokawa, 1992). From these intensity profiles, we made plots of the translocation distance against time (Fig. 7, *A* and *B*) and calculated the translocation rate for each experiment. For example, the translocation rates for the axons shown in Figs. 5 and 6 were calculated to be 43 and 51 μm/h, respectively. The average of the translocation rate from 21 axons showing anterograde movement of bleached spots was 42.5 (±4.2) μm/h. In our previous photoactivation experiments, one of the characteristic features of translocating fluorescence was that the fluorescent zone moved out from its initial position without significant spreading (Okabe and Hirokawa, 1992). This seems to be a feature of photobleached zones as well, since no detectable troughs remained behind the bleached zones on intensity profiles (Figs. 5 *J* and 6 *H*).

Although more than half of the photobleached regions in

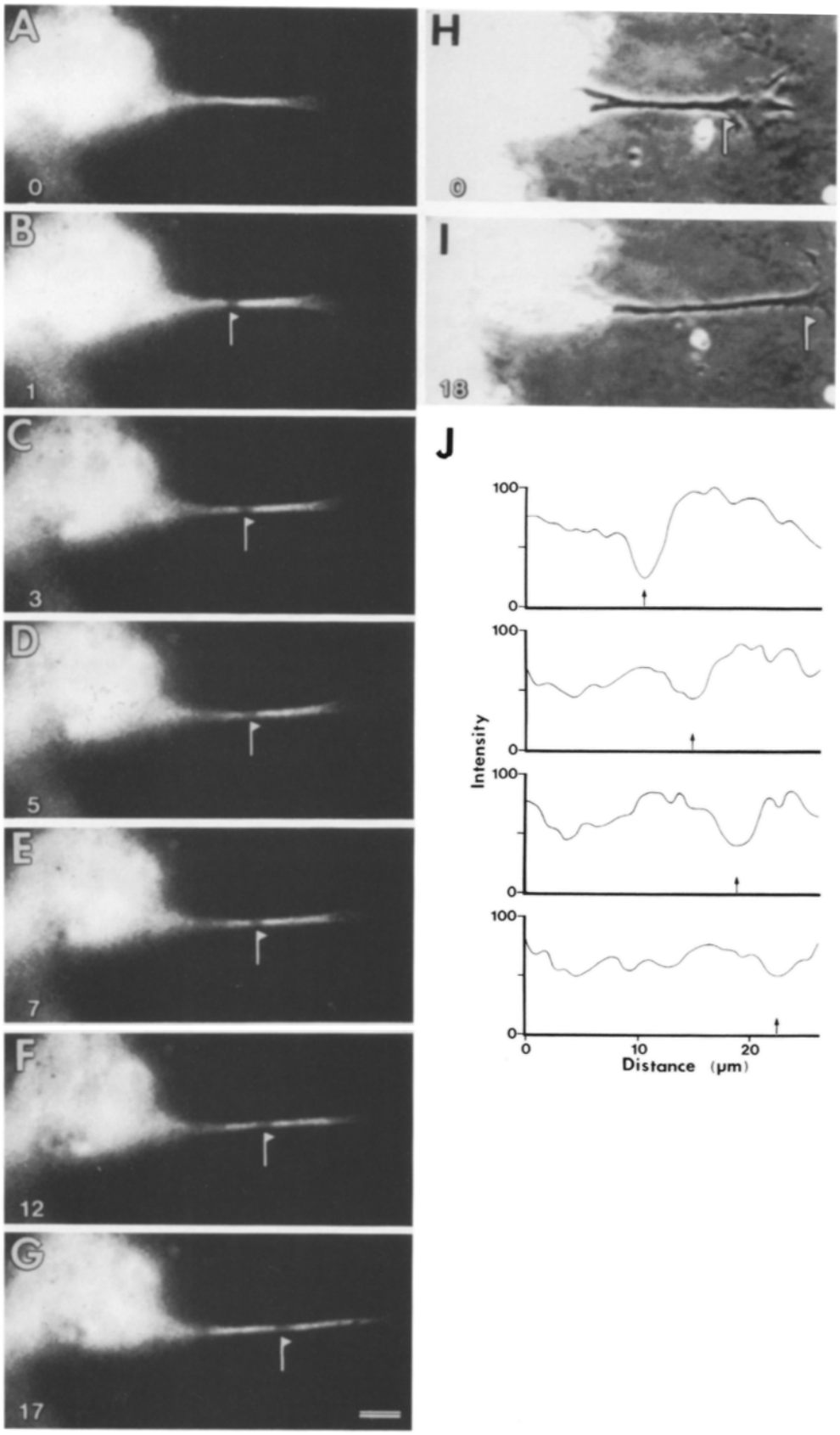

Figure 5. Movement of photobleached MTs at the proximal part of the growing *Xenopus* axon. (*A–G*) A photobleaching run in a growing *Xenopus* neuron. Forward movement of a photobleached zone can be observed (*arrows*). (*H* and *I*) Phase contrast images of the same neuron during the photobleaching run. After photobleaching, significant elongation of the axon was observed (*arrows*). Time in minutes relative to the photobleaching pulse is shown in the lower left-hand corner of each panel. (*J*) Intensity profiles of photobleached regions created from digital images. The bottom of the fluorescence intensity within the bleached zone (*arrows*) moved toward the distal end of neurites (right side of the figure). Time point of each profile is as follows: from top to bottom, 57 s (*B*), 4 min 57 s (*D*), 11 min 57 s (*F*), 16 min 57 s (*G*). Bar, 10 μm.

Xenopus axons showed the anterograde movement, the remaining regions did not move during axonal growth. Fig. 8 shows an example of the stationary bleached spots. During the period of observation, the axon elongated >10 μm. However, no movement of the bleached zone was detected. This was confirmed by creating fluorescence intensity profiles over time, which showed fluorescence recovery without vectorial movement of the trough with time (Fig. 8 *J*).

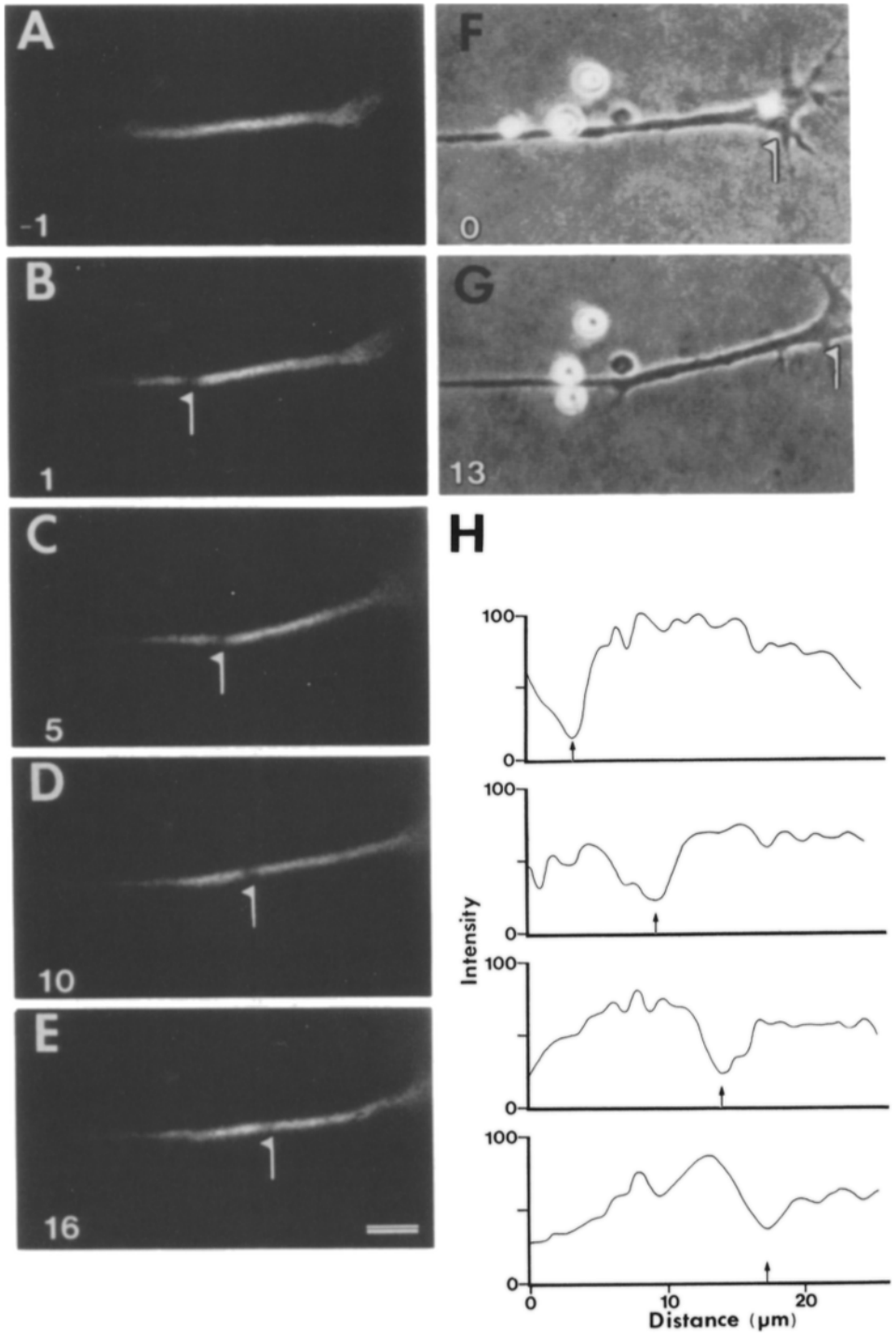

Figure 6. Photobleaching of MTs in the distal part of the growing *Xenopus* axon. (*A–E*) Fluorescent images of photobleached MTs in a growing neurite. Forward movement of a photobleached zone can be observed (*arrows*). (*F* and *G*) Phase contrast images of the same neuron during the photobleaching run. Advancement of the growth cone is observed (*arrows*). Elapsed time (*min*) after photobleaching is shown in the lower left-hand corner of each panel. (*H*) Intensity profiles of photobleached regions created from digital images. The bottom of the fluorescence intensity within the bleached zone (*arrows*) moved toward the distal end of neurites (right side of the figure). Time point of each profile is as follows: from top to bottom, 11 s (*B*), 5 min 2 s (*C*), 10 min 12 s (*D*), 15 min 35 s (*E*). Bar, 10 μm.

Discussion

Fluorescent MTs can be Marked by Photobleaching without Damage In Vitro

The first aim of this study was to determine if fluorescent MTs remained intact when they were bleached sufficiently to distinguish them from non-bleached MTs under a fluorescent microscope. Under the condition we used, MTs labeled with NHS-Fl and stabilized by taxol can be bleached to 30% of their initial fluorescence without causing any structural damage. In as much as MTs bleached to 50% of their initial fluorescence, which can be easily distinguished from non-bleached MTs, were able to be generated with an exposure of 0.1 MJ/m², which was 5–10-fold less than the value which would damage MTs, we conclude that fluorescent MTs can be marked by photobleaching without damage.

Vigers et al. (1988) previously reported that the energy required for near-total photobleaching (~140 MJ/m²) was much more than the total energy required to promote complete dissolution of MTs (2 MJ/m²). This observation seems to be generally consistent with our present data for the following reasons. First, the minimal energy to cause complete MT destruction determined from our experiments was 1.3

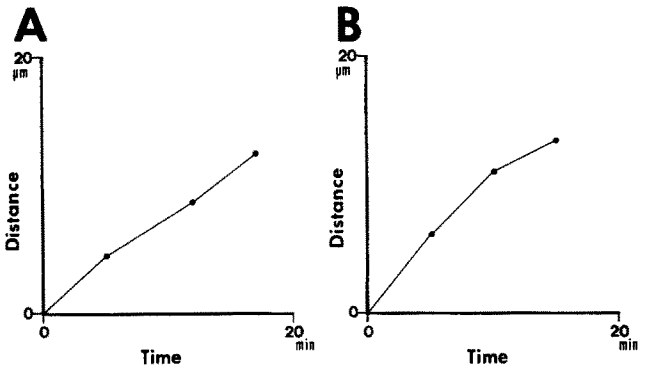

Figure 7. Movement of photobleached zones along the neurites shown in Figs. 5 and 6. From the intensity profiles, the movement of the troughs was plotted against time (*A* for the cell shown in Fig. 5 and *B* for the cell shown in Fig. 6). The average rates of the movement were calculated to be 43 μm/h (*A*) and 51 μm/h (*B*) from these plots.

MJ/m², similar to that reported by Vigers et al. (1988). Second, as we described above, the degree of photobleaching of fluorescent MTs can not be explained by simple first-order reaction, and near-total photobleaching requires much more energy than the value expected from partial photobleaching. For example, since a total light energy of 0.1 MJ/m² is required to bleach 50% of fluorescent tubulin, the theoretical equation predicts that 1 MJ/m² of light energy will reduce fluorescence intensity to $(1/2)^{10}$ = 0.1%. However, our results have shown that the exposure of 1 MJ/m² results in a decrease of fluorescence up to only 20% of the initial value. In this sense, the energy required for near-total photobleaching is expected to be very large, possibly reaching the value (~140 MJ/m²) reported by Vigers et al. (1988).

The mechanism of the progressive increase of stability of the fluorophore to a laser light is not clear. One possibility is that the generation of singlet oxygen molecules by excitation of the fluorophore has some effect on the conversion of the fluorophore to a non-fluorescent state (Kishino and Yanagida, 1988), and that this phenomenon is effective only when fluorophore is concentrated. Alternatively, it may be possible that local heating of MTs with a laser beam converts the fluorophore to the state where it is more resistant to light (Vigers et al., 1988). To settle this point, further experiments under various conditions such as with the removal of oxygen or the addition of oxygen scavengers would be necessary. However, such experiments would deviate from the scope of our present study and were therefore not carried out.

Photobleached MTs Translocate Anterogradely in Xenopus *Neurons*

Since our in vitro experiments have shown that fluorescent MTs can be marked by photobleaching without any detectable damage, we next analyzed the behavior of fluorescent MTs photobleached under similar conditions in growing axons of *Xenopus* neurons. As described in our previous report, fluorescently labeled tubulin injected into *Xenopus* embryos at the two-cell stage can be incorporated into the neuronal cytoskeleton after dissociation and plating of spinal cords from embryos at stages 22–25 (Okabe and Hirokawa, 1992). When a small region of fluorescent axons was illuminated with a laser beam under conditions determined by the in vitro experiments to be harmless to MTs (peak industry of 2.7 MW/m² and exposure time of 1/30 s), a distinct bleach spot was generated on fluorescent axons. Quantification of the digital images of the ICCD camera indicated that the degree of photobleaching of fluorescence under this condition was 10–40% of the initial fluorescence intensity. This value was greater than the degree of photobleaching determined by the in vitro experiments (~50% of the initial fluorescence intensity), suggesting that the conditions of photobleaching are not completely identical in the two systems.

Direct comparison of the present photobleaching conditions with our previous report on mouse neurons (Okabe and Hirokawa, 1990) is difficult because we did not monitor the exact laser output by a laser power meter in our former study. However, we estimate the peak light intensity to be ~6 MW/m² in our previous photobleaching set up, and the exposure can be calculated to be 0.05 MJ/m² (the exposure time = 8 ms). So far, we believe that the photobleaching study on mouse neurons was performed at a similar energy level to the present study. It would be useful if we could discuss our bleaching conditions in relation to those of other groups. However, rhodamine derivatives are generally used as tubulin probes (Gorbsky et al., 1988; Lim et al., 1990; Sammak et al., 1987), and this hampers direct comparison with our fluorescein derivatives. We have not attempted to extensively characterize rhodamine photobleaching since the 514-nm line of an argon ion laser, which is frequently used as a light source for rhodamine bleaching, is not optimal for the excitation of rhodamine fluorophore.

Analysis of the behavior of photobleached MTs revealed frequent anterograde movement of MTs. The frequency of the observed anterograde movement was very similar with photoactivation (15/24 = 63%) (Okabe and Hirokawa, 1992) and photobleaching (21/36 = 58%), supporting the idea that the two methods reported the same biological phenomena. Quantification of the rate of anterograde movement of MTs, however, has shown that the translocation rate of photoactivated MTs (58 ± 11 μm/h [±SEM]) (Okabe and Hirokawa, 1992) is somewhat faster than the rate of photobleached ones (42.5 ± 4.2 μm/h (±SEM)). The reason for this discrepancy is not yet clear, but one possibility is that the photobleaching method still causes some damage to MTs even under the carefully controlled conditions. It may also be possible that some differences in culture conditions might be responsible for the discrepancy in the translocation rates. In this regard, it should be pointed out that the translocation rate of photoactivated MTs reported from another laboratory (38.5 μm/h) (Reinsch et al., 1991) was less than the value for photobleached MTs of our own experiments.

Comparison of the images of the photoactivation and photobleaching experiments also indicates that these two translocation phenomena have almost identical properties. Namely, both photoactivated and photobleached spots moved out from their initial position without significant spreading, resulting in no detectable signal remaining behind the moving mark. Furthermore, the moving marks decayed with time, with a significant loss of signals being observed within the first 20–30-min period. Thus we conclude that the photobleaching method was able to faithfully report the en bloc movement of MTs which was first detected by the photoactivation method.

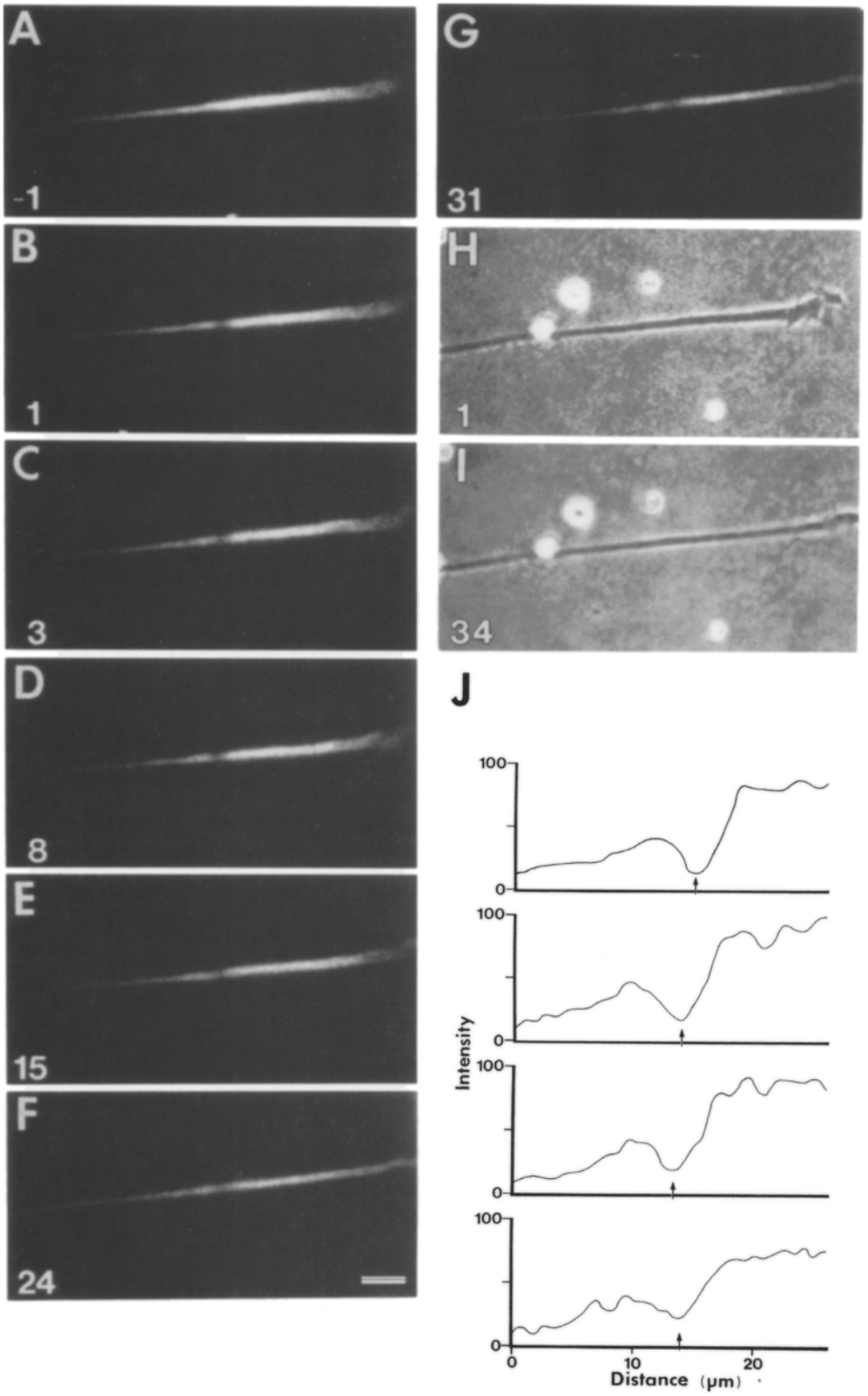

Figure 8. Photobleaching run on a growing *Xenopus* axon showing a stationary nature of the photobleached zone. (*A–G*) Fluorescent images of photobleached MTs in a growing neurite. The photobleached zone did not move significantly during the period of >10 μm elongation of the neurite. (*H* and *I*) Phase contrast images of the growing neurite. (*J*) Intensity profiles of fluorescence across the bleached zone. No anterograde movement of the trough (*arrows*) was observed. Time point of each profile is as follows: from top to bottom, 30 s (*B*), 3 min 2 s (*C*), 8 min 32 s (*D*), 15 min 2 s (*E*). Bar, 10 μm.

Photobleaching Versus Photoactivation

Now we are in the unique position of being able to conduct a direct comparison of the ability and possible pitfalls of both the photobleaching and photoactivation methods. Apparently, a major advantage of the photoactivation method is that we can mark MTs using light at a wavelength that does not excite the released fluorophore. Although it has been postulated that the light energy required to photoactivate a caged fluorophore is several orders of magnitude less than that required to photobleach a fluorophore (Reinsch et al. 1991), we estimated the light energy for photoactivation (0.3 $MW/m^2 \times 0.5\ s = 0.15\ MJ/m^2$) (Okabe and Hirokawa, unpublished observation) to be in the same order as pho-

tobleaching (0.1 MJ/m²). In this sense, the shorter wavelength of light used for photoactivation per se is more likely to damage biomolecules. Indeed, we observed a marked decrease of MT turnover after exposure to a ten-times larger amount of UV light for photoactivation. However, the exposure of photoactivation is easy to control, because the near-total release of the caged fluorophore occurs within an exposure range safe for living samples, and overexposure does not increase the signal but broadens the width of the signal.

A major pitfall of the photobleaching method is that very great light energy is required to produce near-total photobleaching which inevitably damages MTs. Some previous studies which emphasized the potential artifacts of photobleaching (Vigers et al., 1988; Simon et al., 1988) seemed to be based on the inference that near-total photobleaching was necessary to mark MTs. As shown in this study, however, if one carefully controls the extent of photobleaching to be much less than total photobleaching, under such condition the photobleaching method does not break MTs or interfere with the biological process responsible for moving MTs. There are two major advantages of the photobleaching method. One is that the signal from fluorescent MTs is much greater than the signal from photoactivated MTs due to the marked difference in f-to-p ratios of the two preparations. That is to say, the labeling stoichiometry (0.3/dimer) of caged-fluorescein-labeled tubulin is much lower than that of tubulin labeled with NHS-Fl (0.9/dimer). Furthermore, the hydrophobic nature of bis-caged carboxyfluorescein makes it difficult to use this compound for labeling other biological molecules. In this sense, if the analysis of a biological system where the introduction of large amounts of labeled molecules is expected to be difficult would be performed (for example, nerve cells), the application of the photobleaching method would give higher signals. Alternatively, more hydrophilic compounds that are photoactivatable to fluorophores will need to be developed (Theriot and Mitchison, 1991).

Another advantage of the photobleaching method is that visualization of whole tubulin molecules is possible during the experimental runs. This enabled us to judge the distal and proximal ends of MT bundles in the axon precisely and to determine whether a net increase of tubulin molecules occurred within the region distal to the bleached zone. In order to simultaneously monitor MT structures during photoactivation experiments, the co-injection of tubulin labeled with rhodamine is necessary, but this inevitably results in a decrease of the amount of caged-fluorescein-labeled tubulin introduced into cells and hampers the application for cells which are difficult to inject.

In conclusion, we prefer the photoactivation method if both methods can generate signal sufficiently detectable by the available imaging system. However, if the signal from the photoactivated fluorophore is expected to be dim or if the molecule of interest is difficult to be labeled with the caged fluorophore, we would not hesitate to use the photobleaching method, since our effort has shown that, under appropriate conditions, it is able to reveal the behavior of MTs as accurately as the photoactivation method.

This work was supported by a Special Grant-in-Aid for Scientific Research from the Ministry of Education, Science and Culture of Japan, and grants from RIKEN and the Naito Memorial Science Foundation to N. Hirokawa.

Received for publication 30 September 1992.

References

Axelrod, D., D. E. Koppel, J. Schlessinger, E. Elson, and W. W. Webb. 1976. Mobility measurement by analysis of fluorescence photobleaching recovery kinetics. *Biophys. J.* 16:1055–1069.

Black, M. M., and R. J. Lasek. 1980. Slow components of axonal transport: two cytoskeletal networks. *J. Cell Biol.* 86:616–623.

Gorbsky, G. J., P. J. Sammak, and G. G. Borisy. 1988. Microtubule dynamics and chromosome motion visualized in living anaphase cells. *J. Cell Biol.* 106:1185–1192.

Herman, B. 1989. Resonance energy transfer microscopy. *Methods Cell Biol.* 30:219–243.

Hirokawa, N. 1982. Cross-linker system between neurofilaments, microtubules, and membrane organelles in frog axons revealed by the quick-freeze, deep-etching method. *J. Cell Biol.* 94:129–142.

Hirokawa, N. 1991. Molecular architecture and dynamics of the neuronal cytoskeleton. *In* The Neuronal Cytoskeleton. R. D. Burgoyne, editor. Wiley-Liss, New York. 5–74.

Hollenbeck, P. J. 1989. The transport and assembly of the axonal cytoskeleton. *J. Cell Biol.* 108:223–227.

Kellog, D. R., T. J. Mitchison, and B. M. Alberts. 1988. Behavior of microtubules and actin filaments in living Drosophila embryos. *Development.* 103:675–686.

Kishino, A., and T. Yanagida. 1988. Force measurements by manipulation of a single actin filament. *Nature (Lond.).* 334:74–76.

Kreis, T. E., B. Geiger, and J. Schlessinger. 1992. Mobility of microinjected rhodamine actin within living chicken gizzard cells determined by fluorescence photobleaching recovery. *Cell.* 29:835–845.

Lasek, R. J. 1986. Polymer sliding in axons. *J. Cell Sci. Suppl.* 5:161–179.

Lim, S. S., K. J. Edson, P. C. Letourneau, and G. G. Borisy. 1990. A test of microtubule translocation during neurite elongation. *J. Cell Biol.* 111:123–130.

Mitchison, T. J. 1989. Polewards microtubule flux in the mitotic spindle: evidence from photoactivation of fluorescence. *J. Cell Biol.* 109:637–652.

Okabe, S., and N. Hirokawa. 1988. Microtubule dynamics in nerve cells: analysis using microinjection of biotinylated tubulin into PC12 cells. *J. Cell Biol.* 107:651–664.

Okabe,S., and N. Hirokawa. 1989. Axonal transport. *Curr. Opin. Cell Biol.* 1:91–97.

Okabe, S., and N. Hirokawa. 1990. Turnover of fluorescently labelled tubulin and actin in the axon. *Nature (Lond.).* 343:479–482.

Okabe, S., and N. Hirokawa. 1991. Actin dynamics in growth cones. *J. Neurosci.* 11:1918–1929.

Okabe, S., and N. Hirokawa. 1992. Differential behavior of photoactivated microtubules in growing axons of mouse and frog neurons. *J. Cell Biol.* 117:105–120.

Reinsch, S. S., T. J. Mitchison, and M. W. Kirschner. 1991. Microtubule polymer assembly and transport during axonal elongation. *J. Cell Biol.* 115:365–379.

Sammak, P. J., G. J. Gorbsky, and G. G. Borisy. 1987. Microtubule dynamics in vivo; a test of mechanism of turnover. *J. Cell Biol.* 104:395–405.

Sammak, P. J., and G. G. Borisy. 1988*a*. Detection of single fluorescent microtubules and methods for determining their dynamics in living cells. *Cell Motil. Cytoskeleton.* 10:237–245.

Sammak, P. J., and G. G. Borisy. 1988*b*. Direct observation of microtubule dynamics in living cells. *Nature (Lond.).* 332:742–746.

Saxton, W. M., D. L. Stemple, R. J. Leslie, E. D. Salmon, M. Zavortink, and J. R. McIntosh. 1984. Tubulin dynamics in cultured mammalian cells. *J. Cell Biol.* 99:2175–2186.

Schulze, E., and M. Kirschner. 1986. Microtubule dynamics in interphase cells. *J. Cell Biol.* 102:1020–1031.

Schulze, E., and M. Kirschner. 1988. New features of microtubule behavior observed in vivo. *Nature (Lond.).* 334:356–359.

Simon, J. R., A. Gough, E. Urbanik, F. Wang, B. R. Ware, and D. L. Taylor. 1988. Analysis of rhodamine and fluorescein-labeled F-actin diffusion in vitro by fluorescence photobleaching recovery. *Biophys. J.* 54:801–815.

Soltys, B. J., and G. G. Borisy. 1985. Polymerization of tubulin in vivo: direct evidence from assembly onto microtubule ends and from centrosomes. *J. Cell Biol.* 100:1682–1689.

Theriot, J. A., and T. J. Mitchison. 1991. Actin microfilament dynamics in locomoting cells. *Nature (Lond.).* 352:126–131.

Vigers, G. P. A., M. Coue, and J. R. McIntosh. 1988. Fluorescent microtubules break up under illumination. *J. Cell Biol.* 107:1011–1024.